

Quenching Capabilities of Long-Chain Carotenoids in Light-Harvesting-2 Complexes from *Rhodobacter sphaeroides* with an Engineered Carotenoid Synthesis Pathway

Preston L. Dilbeck,[†] Qun Tang,[§] David J. Mothersole,^{||,⊥} Elizabeth C. Martin,^{||} C. Neil Hunter,^{||} David F. Bocian,[§] Dewey Holten,^{*,†} and Dariusz M. Niedzwiedzki^{*,‡}

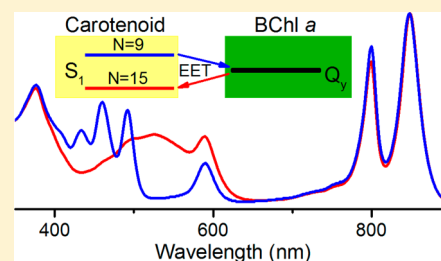
[†]Department of Chemistry, and [‡]Photosynthetic Antenna Research Center, Washington University, St. Louis, Missouri 63130, United States

[§]Department of Chemistry, University of California Riverside, Riverside, California 92521, United States

^{||}Department of Molecular Biology and Biotechnology, University of Sheffield, Sheffield S10 2TN, United Kingdom

Supporting Information

ABSTRACT: Six light-harvesting-2 complexes (LH2) from genetically modified strains of the purple photosynthetic bacterium *Rhodobacter (Rb.) sphaeroides* were studied using static and ultrafast optical methods and resonance Raman spectroscopy. These strains were engineered to incorporate carotenoids for which the number of conjugated groups ($N = N_{C=C} + N_{C=O}$) varies from 9 to 15. The *Rb. sphaeroides* strains incorporate their native carotenoids spheroidene ($N = 10$) and spheroidenone ($N = 11$), as well as longer-chain analogues including spirilloxanthin ($N = 13$) and diketospirilloxanthin ($N = 15$) normally found in *Rhodospirillum rubrum*. Measurements of the properties of the carotenoid first singlet excited state (S_1) in antennas from the *Rb. sphaeroides* set show that carotenoid-bacteriochlorophyll *a* (BChl *a*) interactions are similar to those in LH2 complexes from various other bacterial species and thus are not significantly impacted by differences in polypeptide composition. Instead, variations in carotenoid-to-BChl *a* energy transfer are primarily regulated by the N -determined energy of the carotenoid S_1 excited state, which for long-chain ($N \geq 13$) carotenoids is not involved in energy transfer. Furthermore, the role of the long-chain carotenoids switches from a light-harvesting supporter (via energy transfer to BChl *a*) to a quencher of the BChl *a* S_1 excited state B850*. This quenching is manifested as a substantial (~ 2 -fold) reduction of the B850* lifetime and the B850* fluorescence quantum yield for LH2 housing the longest carotenoids.



INTRODUCTION

The light-harvesting machinery of most photosynthetic purple bacteria is comprised of two types of pigment–protein complexes, LH1 and LH2. Peripheral LH2 absorbs light and transfers excitation energy to inner LH1, which is closely associated with the reaction center.^{1,2} LH2 complexes have circular structures built from identical protein subunits, each of which is a heterodimer of α and β polypeptides spanning a photosynthetic membrane. Each $\alpha\beta$ heterodimer houses three bacteriochlorophyll *a* (BChl *a*) and one carotenoid. The type of carotenoid that is bound to LH2 can vary significantly between bacterial species and habitat (growth conditions). High resolution X-ray structures have been obtained for LH2 from two nonsulfur species, *Rhodopseudomonas (Rps.) acidophila* strain 10050 and *Phaeospirillum (Phs.) molischianum*.^{3–6} Those structures, the 6 Å projection structure of the *Rhodobacter (Rb.) sphaeroides* LH2⁷ and recent electron-microscopy work on LH2 from sulfur purple bacterium *Allochrochromatium vinosum* show that the complexes adopt circular forms with 8–13 $\alpha\beta$ subunits depending on species.^{3–6,8}

All LH2s possess two spectrally distinct forms of BChl *a* designated B850 and B800. B850 is an array of BChl *a*

molecules built from pairs in close contact within each $\alpha\beta$ subunit that have macrocycles perpendicular to the membrane plane. Electronic interactions within a pair and between pairs in the LH2 ring shift the $S_0 \rightarrow S_1$ (Q_y) absorption wavelength to ~ 850 nm. B800 is a monomer-like set of BChl *a* molecules that are oriented parallel to the membrane plane and located between polypeptides of adjacent subunits; their $S_0 \rightarrow S_1$ (Q_y) absorption wavelength is ~ 800 nm.^{3–5}

The main absorption of carotenoids is generally between 400 and 550 nm and is associated with the strongly allowed S_0 ($1^1A_g^-$) \rightarrow S_2 ($1^1B_u^+$) electronic transition. Optical transitions between S_0 ($1^1A_g^-$) and the S_1 ($2^1A_g^-$) lowest singlet excited state are forbidden due to the lack of a change in state symmetry ($g \leftrightarrow u$) and pseudoparity ($+ \leftrightarrow -$).⁹ The negligible transition dipole moment of the S_1 ($2^1A_g^-$) state also implies that variations in carotenoid environment should not significantly affect its excited-state energy or lifetime unless the structure is modified. The energies of both excited states

Received: March 31, 2016

Revised: May 24, 2016

Published: June 10, 2016

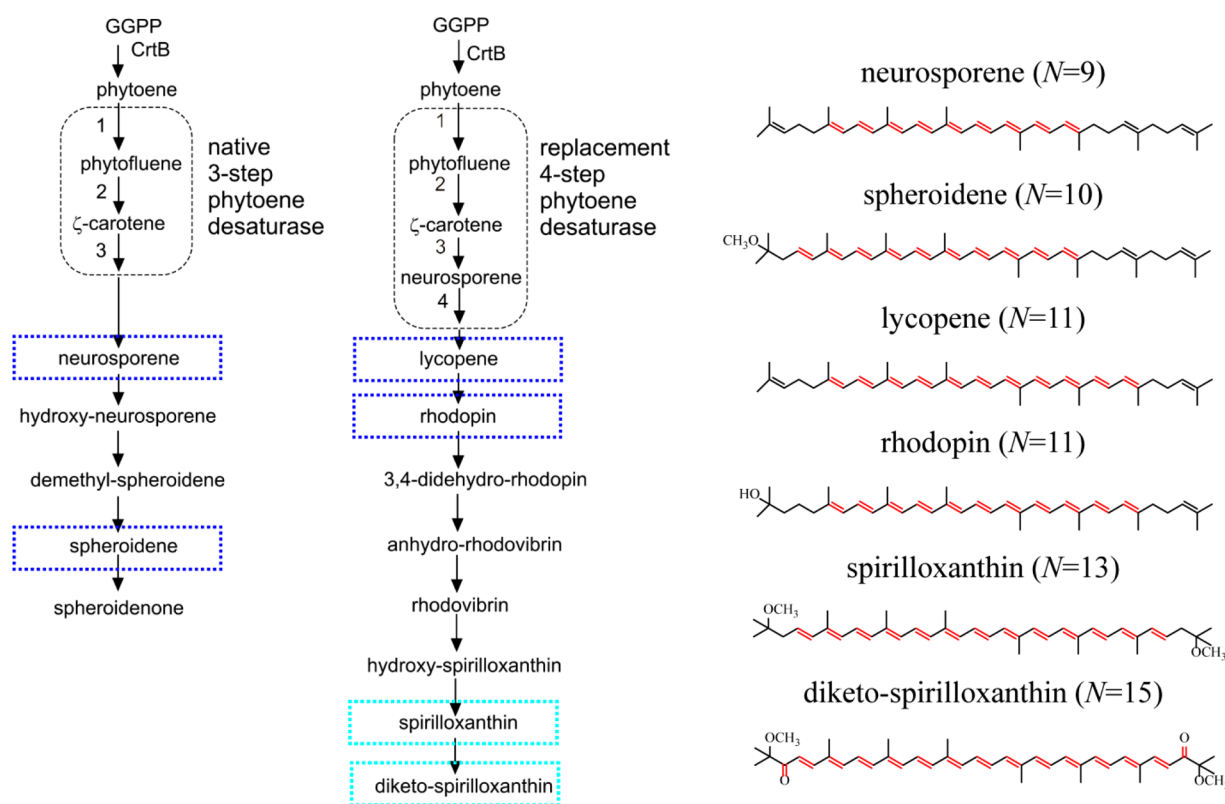


Figure 1. Typical spheroidene/spheroidenone carotenoid biosynthesis pathway and the spirilloxanthin pathway incorporated in the mutant strains. The dashed squared boxes highlight the major carotenoids incorporated into the individual LH2 complexes (blue, the LH2s studied in detail in this research; cyan, the LH2s studied in detail previously²⁴). The chemical structures of carotenoids assembled into the LH2 complexes; red color highlights carotenoid's double bond conjugation, N .

depend on the double-bond conjugation length (N): the more extended the π -electron system, the lower the energy. Prior ultrafast absorption studies of various LH2 complexes showed that although transitions involving the S_1 ($2^1A_g^-$) state are not allowed, this state contributes along with S_2 ($1^1B_u^+$) to the overall yield of energy transfer from carotenoid to B850 ($\Phi_{\text{Car} \rightarrow \text{BChl}}$), especially in LH2s with carotenoids that have modest C=C lengths ($N = 9-10$).¹⁰⁻¹² Herzberg-Teller (vibronic) coupling involving S_2 ($1^1B_u^+$) and S_1 ($2^1A_g^-$) apparently imparts some dipole-allowed character to processes involving S_1 .¹³⁻¹⁶

Carotenoids play a dual role in photosynthetic antenna systems. Carotenoid absorption in LH2 fills the empty spectral window in BChl a absorption between 450 and 550 nm and transfer the absorbed energy to B800 and B850, thereby enhancing overall light harvesting. Carotenoids also serve a photoprotective role by efficiently quenching the triplet excited state of the BChls (B800 and B850) to inhibit formation of reactive oxygen species.^{17,18} Regarding the first role, past studies have shown that $\Phi_{\text{Car} \rightarrow \text{BChl}}$ significantly varies in LH2s among various purple bacterial species. The yields descend from $\sim 95\%$ for LH2s that contain neurosporene ($N = 9$) or spheroidene ($N = 10$)^{10,19-21} to 55–65% for rhodopin, rhodopin glucoside or lycopene ($N = 11$)^{10,19,20} to 30–40% for a mixture of carotenoids ($N = 11-13$),^{22,23} or for spirilloxanthin ($N = 13$), ketospirilloxanthin ($N = 14$, $N_{\text{C}=\text{C}} = 13$, $N_{\text{C}=\text{O}} = 1$) or diketospirilloxanthin ($N = 15$, $N_{\text{C}=\text{C}} = 13$, $N_{\text{C}=\text{O}} = 2$).^{21,24} The relative contributions of $N_{\text{C}=\text{C}}$ and $N_{\text{C}=\text{O}}$ to energy transfer, various S_0 , S_1 , and S_2 properties and effective

conjugation length for long chain carotenoids such as diketospirilloxanthin has been discussed recently.²⁴

The substantial variations in $\Phi_{\text{Car} \rightarrow \text{BChl}}$ suggest (1) not all LH2 proteins have optimal interactions with the carotenoid, (2) not all carotenoids are equally suited to serve dual roles in LH2, or (3) a combination of the above. In the first case, factors by which differing amino acid sequences in the various bacterial species could modulate carotenoid-BChl a electronic communication include structural alteration of interpigment distance and orientation, or purely electronic environmental effects on carotenoid excited-state energy/lifetime, with the latter having electrostatic or specific (e.g., hydrogen-bonding) origin. In the second case, the key is the inherent excited-state properties of the carotenoid dictated by the number and arrangement of C=C and C=O bonds.

Challenges in pinpointing the contributions of the above-noted factors have been considerably ameliorated by recent advances that afford the ability to study a wide range of carotenoids in a common protein environment in a single bacterial species. In particular, genetic engineering of the carotenoid synthesis pathway of *Rb. sphaeroides* has provided LH2s that present a fixed polypeptide architecture and electrostatic milieu housing carotenoids that have N between 9 and 15.^{21,24} In these engineered strains, the native three-step phytoene desaturase (from the spheroidene synthesis pathway) has been replaced by the four-step phytoene desaturase (from the spirilloxanthin pathway),²⁵ along with additional mutations to other enzymes to truncate carotenoid synthesis at a certain conjugation length (Figure 1). Two studies^{21,24} that employ these strains have shown that the overall trend in $\Phi_{\text{Car} \rightarrow \text{BChl}}$

with carotenoid conjugation length N obtained previously using different bacterial species (with different amino acid sequences) is reproduced when employing the common *Rb. sphaeroides* protein scaffolding. The studies have also afforded detailed insights into trends in both ground- and excited-state carotenoid properties with increasing $N_{C=C}$ versus $N_{C=O}$. One conclusion is that variations in $\Phi_{\text{Car} \rightarrow \text{BChl}}$ with carotenoid conjugation length in the various native (or mutant) bacterial species do not arise from substantial peptide-induced alterations in carotenoid properties or carotenoid-BChl a interactions. Thus, future work can focus more tightly on the direct impact of inherent carotenoid characteristics on the details of energy transfer from carotenoid to B800 and B850 and on the subsequent properties of B850*, the terminal singlet excited state in LH2 function.

The studies reported herein complement and extend the prior work on the engineered *Rb. sphaeroides* strains. The static optical studies used to obtain $\Phi_{\text{Car} \rightarrow \text{BChl}}$ for LH2s containing modest-length carotenoids ($N = 9-11$)^{21,24} are joined by time-resolved studies of carotenoid excited-state dynamics employed for strains with the longer analogues ($N = 13-15$)^{21,24}. Additionally, the main focus of the current work is examination, for the entire collection of strains spanning $N = 9-15$, of the excited-state properties of the LH2-bound carotenoids and the BChl a molecules with which they interact. The latter properties include the fluorescence quantum yield and singlet excited-state lifetime of the BChl a array B850. The results are compared with those from prior studies of LH2s that house the same or similar carotenoids within the different protein environments provided by the various bacterial species. Collectively the results extend fundamental insights into carotenoid function in photosynthetic antenna systems.

METHODS AND MATERIALS

***Rb. sphaeroides* Strains and Growth Conditions.** The ΔcrtC , ΔcrtA , $\Delta\text{crtI}::\text{crtI}^{\text{Pa}}\Delta\text{crtC}$, $\Delta\text{crtI}::\text{crtI}^{\text{Pa}}\text{crtD}$, and $\text{crtI}::\text{crtI}^{\text{Pa}}$ strains of *Rb. sphaeroides* were constructed and, except in one case noted below, grown anaerobically (photosynthetically) as described by Chi et al.²¹ After reaching stationary stage the cultures were harvested and pelleted by centrifugation. The primary carotenoids produced by these strains are as follows:^{21,24} ΔcrtC (neurosporene; $N = 9$), ΔcrtA (spheroidene; $N = 10$), $\Delta\text{crtI}::\text{crtI}^{\text{Pa}}\Delta\text{crtC}$ (lycopene; $N = 11$), and $\Delta\text{crtI}::\text{crtI}^{\text{Pa}}\text{crtD}$ (rhodopin, $N = 11$), $\text{crtI}::\text{crtI}^{\text{Pa}}$ when grown anaerobically (spirilloxanthin; $N = 13$, $N_{C=C} = 13$, $N_{C=O} = 0$). When $\text{crtI}::\text{crtI}^{\text{Pa}}$ is grown semiaerobically it gives a mixture of keto-carotenoids including 2-ketoanhydrohodovibrin ($N = 13$, $N_{C=C} = 12$, $N_{C=O} = 1$), 2-ketospirilloxanthion ($N = 14$, $N_{C=C} = 13$, $N_{C=O} = 1$), and 2,2'-diketospirilloxanthin ($N = 15$, $N_{C=C} = 13$, $N_{C=O} = 2$).^{21,24}

Isolation and Purification of LH2. Pellets of bacterial cells were resuspended in 20 mM tris(hydroxymethyl)-amino-methane (Tris) buffer at pH = 8.0. The membranes were released by ultrasonication and then pelleted by centrifugation. Subsequently, the pellet was resuspended in 20 mM Tris buffer (pH = 8.0) to OD₈₅₀ \approx 20 (1 cm path) and mixed with lauryl dimethylamine-oxide (LDAO) to a final concentration of \sim 0.5% for 20 min at room temperature (RT). The insoluble material was pelleted by centrifugation. Final purification of the complexes was carried out using an anion exchange chromatographic column (Q Sepharose High Performance, GE Healthcare) equilibrated with 20 mM Tris buffer (pH = 8.0) with 0.06% LDAO by applying 50 mM gradient steps of NaCl from

150 and 500 mM. The protein-containing fraction was eluted with 300–400 mM NaCl. For comparative purposes LH2 complexes were also purified according to protocol used by Chi et al.²¹ in which the buffer is 4-(2-hydroxyethyl)-1-piperazineethanesulfonic acid (HEPES) and the detergent is n -dodecyl β -D-maltoside (DDM).

Steady-state and time-resolved fluorescence measurements were performed on LH2s from both preparations and tabulated. However, LH2 complexes in the HEPES-DDM show modest variability in B800/B850 ratio (as shown in Chi et al.²¹), perhaps due to slow oxidation of the B800 BChl a that gives rise to modest differences in some photophysical properties. Thus, only results from the Tris-LDAO preparations are used in the figures and detailed discussion of excited-state properties. The only exception is the resonance Raman studies of the LH2-bound carotenoids because they are largely blind to chemical modifications of the B800 BChls.

Steady-State and Femtosecond Transient Absorption Spectroscopy. Time-resolved pump–probe absorption experiments were carried out using a Helios femtosecond transient absorption (TA) spectrometer (Ultrafast Systems LCC, Sarasota, FL) coupled to a Spectra-Physics femtosecond laser system described previously.²³ Excitation wavelengths were preferentially set to excite the first vibronic band of the carotenoid absorption in each case: ΔcrtC (491 nm), ΔcrtA (511 nm), $\Delta\text{crtI}::\text{crtI}^{\text{Pa}}\Delta\text{crtC}$, and $\Delta\text{crtI}::\text{crtI}^{\text{Pa}}\text{crtD}$ (524 nm). The energy of the excitation beam was kept between 200 and 400 nJ for studies at RT, corresponding to an intensity of \sim 0.5–1 \times 10¹⁴ photons/cm². For 77 K studies, in order to minimize permanent photobleaching of the sample, the energy of the pump was lowered to 100 nJ (\sim 3 \times 10¹³ photons/cm²). All steady-state absorption measurements were performed using a Shimadzu UV-1800 spectrophotometer. The absorbance of the samples at the maximum of carotenoid absorption band was set between 0.1 and 0.5 in a 2 mm cuvette (depending on the availability of sample). For low-temperature measurements, the buffered-LH2 solution was mixed with glycerol in 1:1 (v/v) ratio, transferred to a 1 cm square plastic cuvette and frozen in a VNF-100 liquid nitrogen cryostat (Janis, Woburn, MA).

Steady-State Fluorescence Spectroscopy. Fluorescence and fluorescence–excitation spectra were recorded at RT using a Horiba-Spex Nanolog fluorometer. The spectra were recorded with detection at 90° to excitation and corrected for the instrument spectral response. The excitation and detection bandwidths were 2–4 nm. To avoid front-face and inner-filter effects, the samples were adjusted to an absorbance \leq 0.1 at the excitation and emission wavelengths. Fluorescence quantum yields (Φ_f) were determined by comparing the integrated absorbance-corrected emission spectrum to that for free base tetraphenyl porphyrin ($\Phi_f = 0.09$ in degassed toluene and 0.07 in nondegassed toluene²⁶) excited at the same wavelength; data were acquired using excitation at in the BChl a Soret (375 nm) and Q_x (590 nm) bands and averaged. The efficiency of carotenoid-to-bacteriochlorophyll energy transfer ($\Phi_{\text{Car} \rightarrow \text{BChl}}$) was obtained from the ratio of the amplitudes of the carotenoid features in the B850 fluorescence–excitation spectrum to those at the same wavelengths in the absorbance spectrum after normalizing at the Q_y maximum (\sim 850 nm).

Resonance Raman (RR) Spectroscopy. The RR spectra were obtained at RT of the isolated carotenoids in tetrahydrofuran (THF) and of the LH2 complexes resuspended either in Tris-LDAO or HEPES-DDM solution as described

previously.²⁴ Briefly, the RR spectra were acquired with a Spex 1877 triple spectrograph (Horiba, Japan) equipped with holographically etched 1800 groove/mm gratings in the third stage and UV-enhanced charge-coupled device (EUV1152-UV; Princeton Instruments). The excitation wavelength of 532 nm was provided by Verdi-V6, diode-pumped solid-state laser (Coherent) with power set to 5–6 mW and a beam diameter of ~ 0.5 mm. The scattered light was collected at 90° using a 50 mm $f/1.4$ Cannon camera lens. The spectra were acquired with 1–2 h of signal averaging (20×180 s to 40×180 s scans). The spectral resolution was ~ 2 cm^{-1} at a Raman shift of 200 cm^{-1} . The spectra data were calibrated using the known frequencies of indene.

Time-Resolved Fluorescence Spectroscopy. The time-correlated single photon counting (TCSPC) setup consisted of a stand-alone Simple-Tau 130 system (Becker&Hickl, Germany), equipped with the following: a PMC-100–20 detector (GaAs version) that has an instrument response function (IRF) with a full width at half-maximum (fwhm) of <200 ps, a PHD-400 high speed Si pin photodiode (as triggering module), a motorized Oriel Cornerstone 130 1/8 m monochromator (Newport) with manually controlled, micrometer-adjustable entrance and exit slits and ruled 1200 1/mm grating blazed at 750 nm (having spectral resolution of 21 nm with fully open entrance slit), and a manual filter wheel. Excitation pulses at 590 nm were produced by an Inspire100 ultrafast optical parametric oscillator (Spectra-Physics) pumped with Mai-Tai, an ultrafast Ti:sapphire laser (Spectra-Physics), generating ~ 90 fs laser pulses at 820 nm with a frequency of 80 MHz. The frequency of the excitation beam was lowered to 8 MHz (125 ns between excitations) by a 3980 Pulse Selector equipped with a 3986 controller (Spectra-Physics). Isotropic excitation of the sample was achieved by depolarizing the excitation beam using an achromatic depolarizer (DPU-25, Thorlab). The intensity of excitation beam (focused to an ~ 1 mm circular spot at the sample) was set to $\sim 10^{10}$ photons/ cm^2 per pulse to ensure annihilation-free conditions. The signal was recorded at 90° to the excitation. The LH2 complexes were suspended in the appropriate buffer-detergent solution to an absorbance of ≤ 0.1 in the B850 band.

Data Processing and Fitting. Group velocity dispersion in the TA data sets was corrected using Surface Explorer Pro software provided by Ultrafast Systems by building a dispersion correction curve from a set of initial times of transient signals obtained from single wavelength fits of representative kinetics. Kinetic modeling (global analysis) of TA data was performed using CarpetView (Light Conversion Ltd., Vilnius, Lithuania). The instrument temporal response function was assumed to have a Gaussian-like shape with the fwhm of 150–250 fs and was used as a fixed parameter in the fitting procedure. The focus of the analysis was to obtain trends in the photophysical characteristics of the carotenoids and BChls for the various LH2s. Thus, a method commonly used for global analysis of TA data for LH2 complexes was employed in which the time evolution of the system is described by a sequential series of steps following photoexcitation. The spectral components thereby obtained are typically called evolution associated difference spectra (EADS).²⁷ The EADS typically may not correspond to the spectra of the true transient states but provide useful information on the time evolution of the system.

RESULTS

Static Absorption Studies. The RT and 77 K absorption spectra of the LH2 complexes from four (of six) *Rb. sphaeroides* strains are shown in Figure 2A, C, E, and G. At RT, the B800

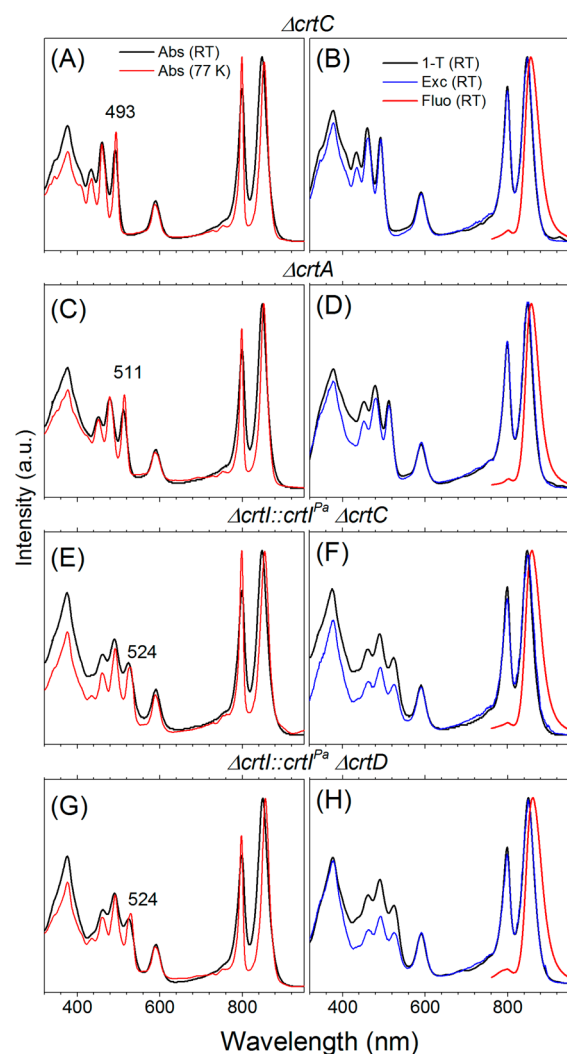


Figure 2. Steady-state absorption spectra of the LH2 complexes recorded at RT and at 77 K (left column). Absorbance (1–T), fluorescence excitation, and fluorescence spectra of the LH2 complexes recorded at RT (right column).

maximum is at 800 nm in all of the complexes, while the B850 peak position shows a small variation between 848 and 850 nm (Table 1). Upon lowering the temperature to 77 K, a bathochromic shift of ~ 4 nm of the B850 band is seen in all cases (Table 1). The B800/B850 peak-intensity ratio varies between 0.7 and 0.8 at RT, a typical range for properly assembled LH2 complexes.^{10,28} Although the carotenoid absorption reveals a clear vibronic structure at RT, lowering the temperature to 77 K substantially enhances resolution of the vibronic bands. Temperature also affects the B800/B850 amplitude ratio, increasing to ~ 1 for some complexes at 77 K.

A point relevant to analysis of carotenoid function in LH2 is whether binding to the protein affects the structure of a carotenoid relative to organic solvents. Such distortion would likely influence the vibronic-progression profile. Thus, comparison of the absorption spectrum of a protein-bound and

Table 1. Spectroscopic Properties of BCChs (B850) and Primary Carotenoids in LH2 Complexes Studied Here and Previously

Rb. sphaeroides strain (other species)	primary carotenoids (%) ^a	N ^b	N _{C=C}	N _{C=O}	Car S ₂ (0-0) ^c (nm) RT ^g	Car S ₂ (0-0) ^c (nm) 77 K (10 K)	B850 (nm) RT	B850 (nm) 77 K (10 K)	τ_F (ns) ^d LDAO (DDM) ^h	Φ_F^{de} (%) LDAO (DDM)	$\Phi_{Car \rightarrow B850}$ LDAO (DDM)	ref
$\Delta crtC$	neurosporene (100)	9	9	0	492	493	847	853	1.33 (0.86)	10.7 (9.7)	87 (94)	this work 21
(G1C)	neurosporene (100)	9	9	0	492	(494)	847	(854)			91	10
$\Delta crtA$	spheroidene (96)	10	10	0	511	514	848	851	1.38 (1.13)	11.0 (8.5)	88 (96)	this work 21
wild type	spheroidene (100)	10	10	0	511	(515)	848	(852)	1.8 ^f 1.0 0.98 0.93		93	10 29 30 31 32
$\Delta crtI::crtI^{\Delta}$ $\Delta crtC$	lycopene (91)	11	11	0	524	527	848	854	1.1 (0.76)	8.5 (7.5)	66 (64)	this work 21
(DPF240[pERW12])	lycopene	11	11	0	526						~55	33
$\Delta crtI::crtI^{\Delta}$ $\Delta crtD$	rhodopin (26), lycopene (34), MeO/OH-lycopenes (36)	11	11	0	524	529	849	856	1.1 (0.8)	8.1 (6.8)	65	this work
(Rps. acidophila 10050)	rhodopin glucoside (100)	11	11	0	524	(529)	856	(868)			(62) 54	21 10
$\Delta crtI::crtI^{\Delta}$ (PS) ^g	spirilloxanthin (71)	13	13	0					1.0 0.89 (0.77)	5.5 (6.2)	46 (39)	this work 21
$\Delta crtI^{\Delta}$ (SA) ^k	diketospirilloxanthin (62) Ketospirilloxanthin (16)	15 14	13 13	2 1	555 <i>nr.</i> ^l	556	849	852	0.74 (0.71)	4.8 (5.7)	41 (35)	24 this work 21

^aFrom Chi et al.²¹ ^bTotal number of conjugated double bonds ($N = N_{C=C} + N_{C=O}$). ^c(0-0) S₀ → S₂ absorption band. ^dB850 excited-state lifetime from fluorescence decay. ^eB850 fluorescence quantum yield. ^fCarotenoid-to-BCCh α energy transfer efficiency from excitation vs absorbance (1-T) spectra. ^gRoom temperature. ^hLDAO vs DDM preparations. ⁱAt 6 K. ^jPhotosynthetically (anaerobically) grown. ^kSemiaerobically grown. ^lNot resolved.

solvent-dissolved carotenoid should give insights into potential structural differences. This point was explored as described in detail below.

The pigment complement of each LH2 complex studied here was analyzed previously.²¹ The carotenoid content in most cases was found to be relatively simple and consist primarily of a single carotenoid (Table 1). The $\Delta crtI::crtI^{\Delta} crtD$ LH2 is more complex and contains several carotenoids with similar absorption spectra; these carotenoids have the same number of conjugated C=C bonds ($N_{C=C} = 11$; Table 1). Consequently, if the protein does not distort the carotenoid backbone, the carotenoid absorption profile in LH2 should be mimicked by the (the sum of) absorption spectra of individual carotenoids in solution. The spectra should only differ by a general wavelength shift due to the higher polarizability of protein binding pocket. Such a situation is demonstrated in Figure 3 for representative

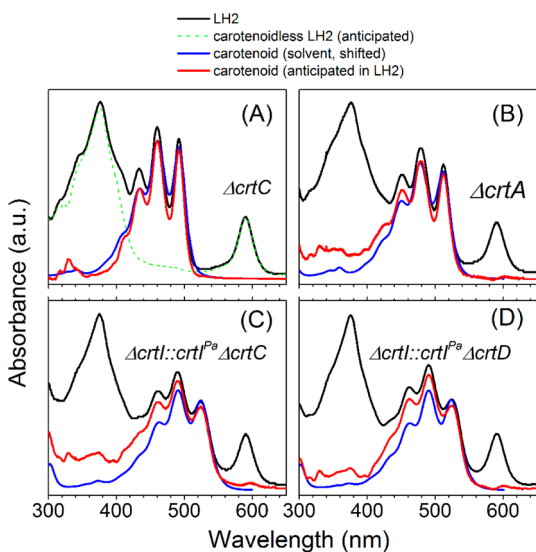


Figure 3. Reconstruction of the carotenoid absorption band in the absorption spectra of the LH2 complexes. The black line represents the LH2 absorption; the blue line is the carotenoid absorption spectrum taken in acetonitrile/THF solvent mixture; the green dashed line is an anticipated absorption spectrum of a carotenoidless LH2.²⁴ The red profiles are predicted absorption spectra of the carotenoids bound into the LH2s.

LH2 samples. The expected absorption spectrum of the LH2-bound carotenoid was obtained by subtraction of the projected absorption of the LH2-bound BChl *a*, as was done previously (dashed green line in Figure 3A).²⁴ The resulting spectra (red lines) track the absorption spectra of the primary carotenoids in acetonitrile (blue line), which have been shifted by $\sim 1000 \text{ cm}^{-1}$ to lower energy (longer wavelength). In the case of spheroidene, lycopene, and rhodopin (Figure 3B–D) the spectra in the LH2s are more intense in the UV versus the level predicted from the spectra in organic media, most likely due to light scattering in the protein solution. Overall, the good agreement between carotenoid absorption spectra in LH2 and the organic solvent, together with the similar $\sim 1000 \text{ cm}^{-1}$ energy shift of the latter in all cases, is strong evidence that the overall carotenoid structure is preserved. The implication of this finding is that any differences observed in excited-state properties of the carotenoids in LH2 versus organic media arise primarily from energy transfer to the BChls rather than

differences in the effects of protein binding on carotenoid structure.

RR Studies. Detailed information concerning potential structural changes in the carotenoid geometry upon incorporation into the LH2 protein were examined via RR spectroscopy. In this regard, a useful marker of carotenoid conjugation length is the ν_1 band (near 1500 cm^{-1}) that arises from the stretching modes of C=C bonds. It is known that the wavenumber position of the ν_1 band has a specific relationship with the carotenoid conjugation length (N).^{35–38}

Figure 4A compares the RR spectra of the isolated carotenoids in THF solution and LH2 complexes. The position of ν_1 for the protein-bound carotenoids is generally shifted to lower energies by $3\text{--}6 \text{ cm}^{-1}$. In addition, the results obtained for the LH2s with spirilloxanthin and diketospirilloxanthin demonstrate that different detergent treatments applied during protein purification process (LDAO versus DDM) have negligible effect on the carotenoid structure.

Previous studies of several open chain carotenoids have shown that the wavenumber of ν_1 in the RR spectrum and that of the (0–0) vibronic band in the steady-state absorption spectrum have an approximately linear correlation.³⁷ Figure 4B shows this correlation for a set of carotenoids studied in THF solution. Because the energy of the S_2 ($1^1B_u^+$) state is also a linear function of reciprocal of carotenoid conjugation ($1/N$), the energy of the ν_1 mode should also linearly depend on $1/N$. This is shown in Figure 4C. This relation is presented for carotenoids in THF solutions and in the LH2 complexes. The LH2 with diketospirilloxanthin is omitted because previous studies have shown that the carotenoid composition is complex and that the RR feature is the sum of the ν_1 modes of several carotenoids with various N .²⁴

The above results show that the energy of the ν_1 mode is indeed a linear function of $1/N$ in both solvent and protein environments; moreover, the lines for the carotenoids in the protein and organic solvent are parallel. This finding implies that the energetic shift of the ν_1 mode is the same for all the carotenoids and thus, most likely results from the effect of increasing medium polarizability. Therefore, upon binding to the protein, the effective conjugation of all the carotenoids remains unchanged from organic media, otherwise the two linear functions would not be parallel.³⁷

Static Fluorescence and Fluorescence–Excitation Studies. The fluorescence spectrum of each *Rb. sphaeroides* LH2 (in Tris-LDAO) was measured using excitation in the BChl Soret band (385 nm) and Q_x band (590 nm). The fluorescence spectra (590 nm excitation) are shown in Figure 2. Emission is observed predominantly from the BChl *a* array B850 with a maximum in the range 856–862 nm. The spectra are basically the same as those found previously for these LH2s in HEPES-DDM.²¹

The fluorescence–excitation spectra (Figure 2) were obtained upon monitoring emission on the long-wavelength side of the B850 fluorescence band. These spectra are accompanied by $1-T$ spectra and normalized at the $\sim 850 \text{ nm}$ maximum, a wavelength for which the B850 BChls are excited directly and exclusively. Comparison of the amplitudes of the normalized fluorescence–excitation spectra and $1-T$ spectra in the region of the carotenoid absorption gives a measure of $\Phi_{\text{Car} \rightarrow \text{BChl}}$ for each LH2. It is evident from Figure 2 that $\Phi_{\text{Car} \rightarrow \text{BChl}}$ decreases as the double-bond conjugation length (N) of the carotenoid increases. This finding is in agreement with previous results for the same or similar carotenoids in LH2

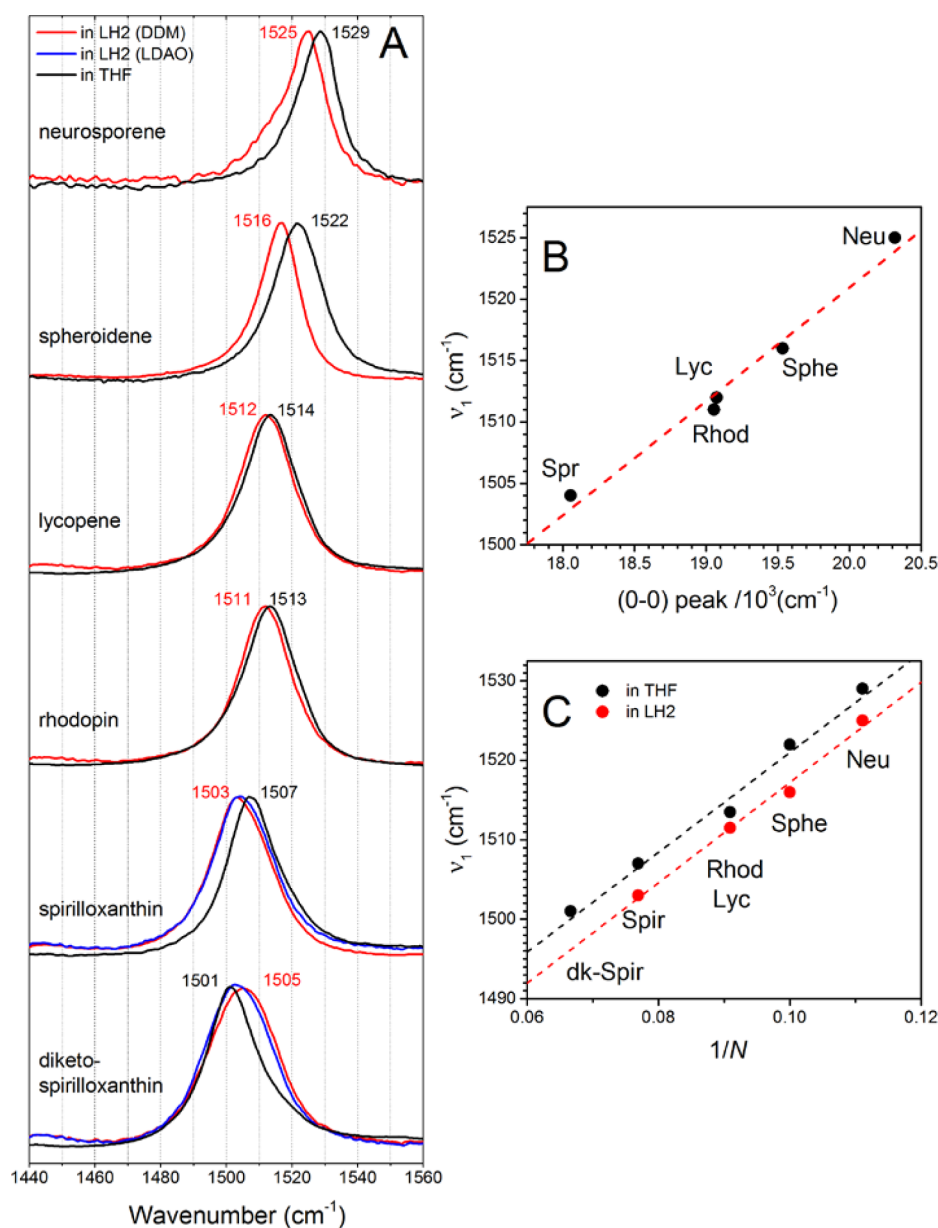


Figure 4. RR characteristics of the LH2-bound and solvent dissolved carotenoids: (A) Spectra of the individual carotenoids in the region of the ν_1 mode taken observed for the LH2s and in THF upon excitation at 532 nm. (B) ν_1 mode as a function of the (0–0) vibronic band of carotenoid in LH2 (C) Comparison of the relation between ν_1 mode and nominal double bond conjugation (N) for carotenoids dissolved in THF and bound in LH2s.

from various bacterial strains (Table 1).^{10,19–21,24,39,40} The effect has been attributed to two factors: a reduced carotenoid-BChl a spectral (energy) overlap and enhanced internal conversion of the excited carotenoid to the ground state. With increase of carotenoid conjugation, the relevant excited states become closer in energy to the ground state and internal conversion becomes progressively more rapid (in agreement with energy gap law for nonradiative decay) and at some point may become competitive with energy transfer.

The quantum yield of fluorescence (Φ_f) from excited B850 (B850*) was also measured for each *Rb. sphaeroides* LH2 at RT. Samples were excited in the Soret (375 nm) and Q_x (590 nm) bands and the values averaged (Table 1). The Φ_f values of 10.7–11.0% for strains $\Delta crtC$ and $\Delta crtA$ that incorporate neurosporene ($N = 9$) and spheroidene ($N = 10$), respectively, are comparable to the $\Phi_f = 9.9\%$ reported for *Rb. sphaeroides*

WT,³¹ which appears to be the sole value for an LH2 in the literature. The Φ_f values drop to 8.1–8.5% for the strains ($\Delta crtI::crtI^{Pa}\Delta crtC$ and $\Delta crtI::crtI^{Pa}\Delta crtD$) that produce primarily lycopene and/or rhodopin ($N = 11$). The values drop further still to 5.5% for strain $\Delta crtI::crtI^{Pa}$ grown photosynthetically that produces primarily spirilloxanthin ($N = 13$) and to 4.8% for the same strain grown semiaerobically with incorporation of significant diketospirilloxanthin ($N = 15$). Thus, increasing conjugation length of the carotenoid not only reduces the efficiency of energy transfer from carotenoid to B850 ($\Phi_{Car \rightarrow BChl}$), but also a property (Φ_f) of the B850* excited state that is produced. The next section describes further exploration of both facets of LH2 functionality via time-resolved studies.

TA Studies. Femtosecond-time-resolved absorption studies were performed to obtain more detailed information on the

carotenoid S_1 ($2^1A_g^-$) excited state, particularly its lifetime in the various LH2s (versus in organic media). Such information provides additional information on carotenoid-to-BChl a energy transfer.

The left column of Figure 5 shows the TA spectra of the LH2s taken at different delay times in the VIS spectral range at

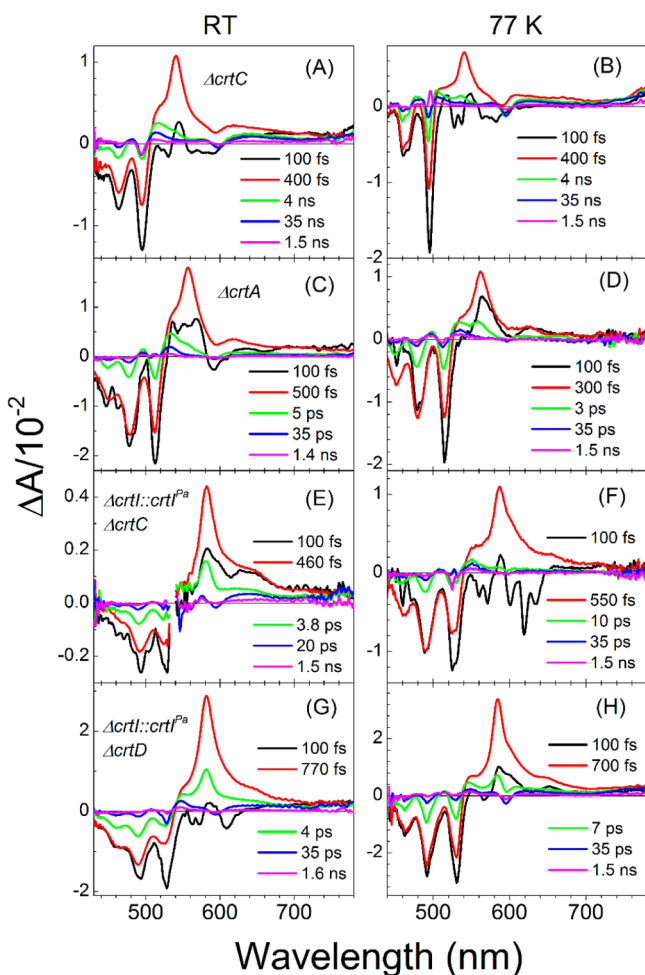


Figure 5. TA spectra of the LH2 complexes in the VIS spectral range upon excitation at their carotenoid band. The spectra were recorded at various delay times after excitation and taken at RT (left column) and at 77 K (right column).

RT. The samples were excited into the carotenoid (0–0) vibronic band (Table 1). The early time 100 fs TA spectra show characteristic features associated with the S_2 ($1^1B_u^+$) state of the carotenoid—bleaching of the ground-state absorption band (GSB), appearing simultaneously with a weak S_2 ($1^1B_u^+$) \rightarrow S_0 ($1^1A_g^-$) stimulated emission.

A couple hundred of femtoseconds after the initial appearance of the GSB, an excited-state absorption (ESA) of the carotenoid S_1 ($2^1A_g^-$) state emerges. It is visible as a pronounced feature with maximum at 540 nm for $\Delta crtC$, 557 nm for $\Delta crtA$, 580 nm for $\Delta crtI::crtI^Pa \Delta crtC$ and at 581 nm for $\Delta crtI::crtI^Pa crtD$. The S_1 ($2^1A_g^-$) \rightarrow S_n ESA band disappears within a few picoseconds, seemingly more quickly in the LH2s that contain carotenoids with shorter C=C conjugation, such as neurosporene and spheroidene. Subsequent to the decay of the S_1 ($2^1A_g^-$) \rightarrow S_n ESA band, the remaining spectral features associated with the carotenoids show some characteristics

resembling those of the so-called carotenoid S^* state, previously suggested to be a precursor of the carotenoid triplet state.^{10,41–43} Lowering the temperature to 77 K impacts the TA spectra of the LH2-bound carotenoids in several ways. In all cases except $\Delta crtC$, the position of the S_1 ($2^1A_g^-$) \rightarrow S_n ESA band shifts bathochromically by 3–6 nm and its amplitude relative to the GSB feature decreases.

The temporal characteristics of carotenoid (and BChl a) excited states were investigated by applying global analysis of the TA data sets. As described in the Methods and Materials section, the data were fit assuming a sequential kinetic model for the excited-state evolution to give EADS.²⁷ Although EADS are typically not those of the true states (species) involved the spectral evolution and EADS associated with the S_1 ($1^1A_g^-$) excited state can be easily recognized as is dominated by the S_1 ($1^1A_g^-$) \rightarrow S_n ESA band. This type of global analysis was applied to the data sets depicted in Figure 5. The EADS from analysis of RT TA data are given in Figure 6. The left column shows EADS for each LH2, the right column shows corresponding EADS concentrations, matched by the same

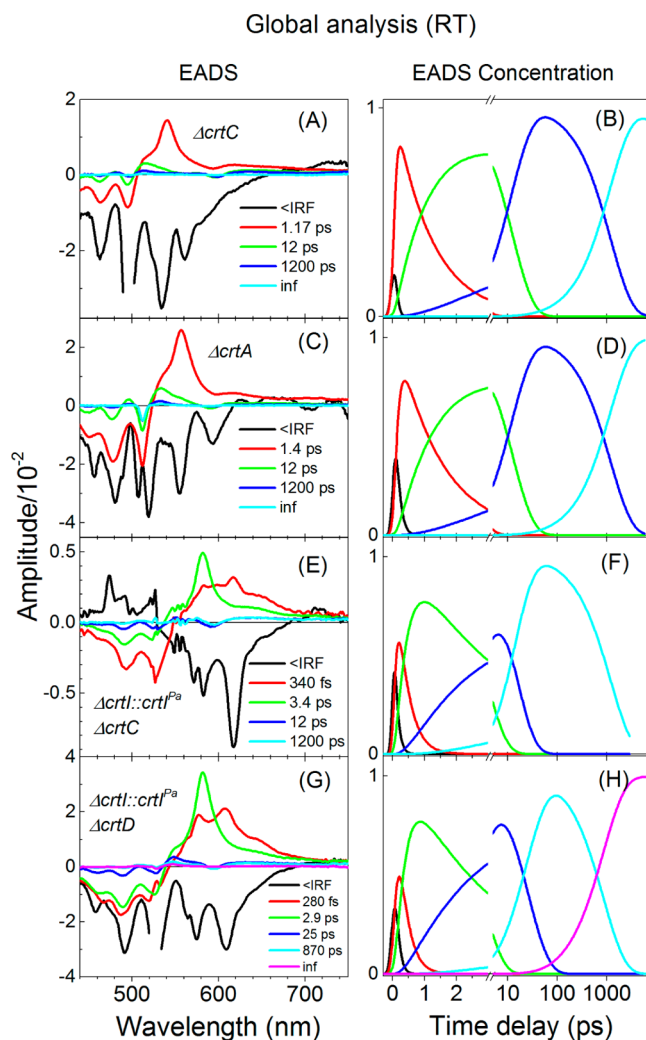


Figure 6. Global analysis results of the RT TA data sets given in Figure 5. The fitting applied a sequential model of the excitation decay path and gives EADS with the corresponding decay lifetimes (left column). The contribution of a particular EADS in the raw TA spectrum at a certain delay time is given by the EADS concentration (right column).

color. The fitting required either 5 or 6 EADS to obtain satisfactory fits.

The first EADS with the lifetime marked as <IRF (shorter than the fwhm of the IRF) corresponds to the initial GSB and the S_2 ($1^1B_u^+$) \rightarrow S_0 ($1^1A_g^-$) stimulated emission, appearing up to 650 nm. The EADS time constant corresponds to the lifetime of the S_2 ($1^1B_u^+$) state, but the value is obscured by both the instrument time resolution and interference from strong solvent/buffer contribution (stimulated Raman bands, etc.). The EADS with 280–340 fs time constant, which is not observed in the LH2s with spheroidene and neurosporene, shows spectral and temporal characteristics of the ESA from a vibrationally nonequilibrated S_1 ($2^1A_g^-$) state, commonly called a hot S_1 . The EADS with a lifetime ranging from about 1.2 to 3.4 ps is associated with decay of the vibrationally equilibrated S_1 ($2^1A_g^-$) state. The spectral profile of this EADS is dominated by the carotenoid S_1 ($2^1A_g^-$) \rightarrow S_n ESA band. The EADS with a lifetime of 12–25 ps has been previously assigned to the enigmatic carotenoid S^* state.^{10,41–43} The next EADS with lifetime of 870–1200 ps is associated with excited state of the B850 BChls (B850*). This contribution results mostly from bleaching of the weak BChl a Q_x band at \sim 590 nm; because the amplitude is small, the time constant should be considered as only a rough measure of the B850* lifetime. The latter has been investigated in detail by monitoring the B850* fluorescence decay via TCSPC (see Table 1 and results below). The EADS with infinite lifetime corresponds to a very small signal in the region of carotenoid absorption and is most likely associated with carotenoid triplet state.

Global analysis results of the TA data sets obtained at 77 K are shown in Figure 7. The analysis does not reveal kinetic components associated with the hot S_1 state for the LH2 complexes from $\Delta crtI::crtI^{Pa}\Delta crtC$ and $\Delta crtI::crtI^{Pa}crtD$ strains. In addition, unlike what is typically observed for isolated carotenoids in frozen solvent glasses (Table 2),^{44,45} the S_1 ($2^1A_g^-$) state lifetime differs only marginally at 77 K versus RT.

Time-Resolved Fluorescence Studies. The excited-state lifetime of the B850 BChls was obtained via fluorescence decay profiles obtained using weak (nonamplified) excitation pulses and TCSP detection. This technique was employed to avoid any potential effects on the B850* decay profile from exciton annihilation arising from the (moderately) intense excitation pulses (from an amplified laser) used for TA measurements. The profiles for B850* fluorescence decay for the LH2 series are given in Figure 8. The major carotenoids present in each complex are provided on the internal figure legend and the full complement for the given *Rb. sphaeroides* strain in Table 1.

DISCUSSION

The spectroscopic studies reported herein afford detailed insights into how the protein environment influences the properties of the carotenoids and how carotenoid structure influences the energy transfer characteristics of the LH2 complexes. Two key points that emerge are that (1) the properties of the polypeptide have minimal influence on regulating the electronic communication between the carotenoids and BChls and (2) carotenoids with long conjugation lengths quench B850*. These issues are discussed in more detail below.

The present study in conjunction with prior studies of the engineered *Rb. sphaeroides* strains^{21,24} shows that the precipitous drop in the carotenoid-to-BChl a energy transfer efficiency, which has been observed for LH2 complexes from

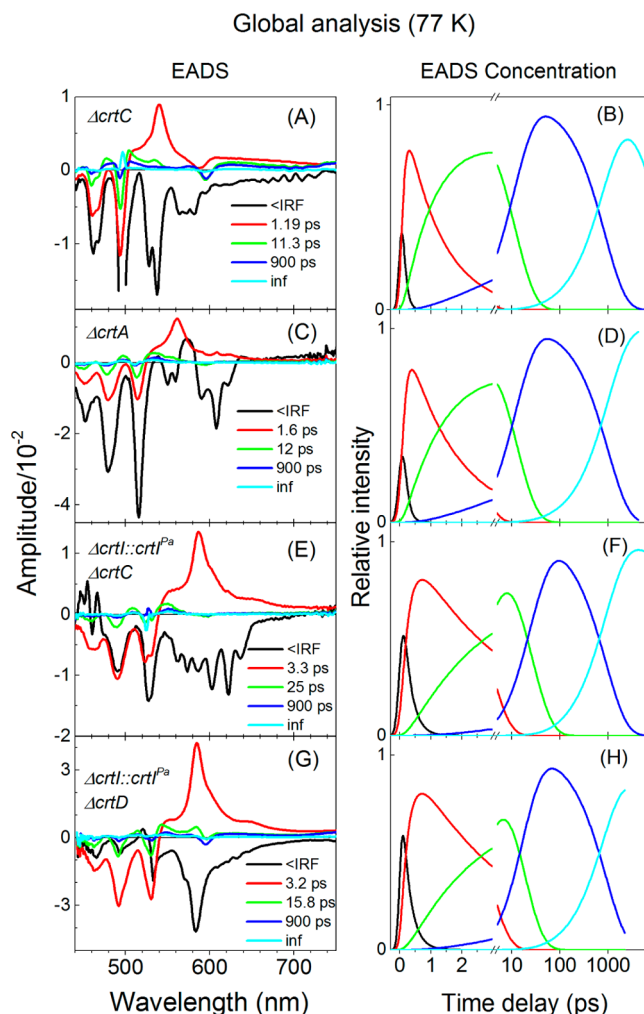


Figure 7. Global analysis results of 77 K TA data sets given in Figure 5. The fitting applied a sequential model of excitation decay path and gives EADS with corresponding decay lifetimes (left column). The contribution of a particular EADS in the raw TA spectrum at a certain delay time is given by the EADS concentration (right column).

various bacterial species that bind longer-conjugation carotenoids, is underpinned by the electronic properties of the carotenoid. Specifically, the energy of the carotenoid S_1 ($2^1A_g^-$) state relative to that of B850* (and B800*) regulates the rate and yield of energy transfer from the former to produce the latter. The lifetime of the S_1 ($2^1A_g^-$) state, which is sensitive to the rate and yield of energy flow to the BChls, is essentially the same in LH2s from various bacteria housing the same carotenoid, including the engineered *Rb. sphaeroides* strains studied here. These conclusions are supported by the $\Phi_{Car \rightarrow BChl}$ values across the LH2s, which measure the extent of energy transfer to B850 from both the carotenoid S_1 ($2^1A_g^-$) and S_2 ($1^1B_u^+$) states. Therefore, differences in polypeptide properties are not a significant contributor to regulation of energy flow from carotenoid to the BChls in LH2 complexes.

Detailed knowledge about the S_1 ($2^1A_g^-$) excited state lifetime of each carotenoid in solvent and in the LH2 complex (Table 2) allows the efficiency of energy transfer to B850 from S_1 ($2^1A_g^-$) to be estimated from eq 1.

$$\text{Eff}_{\text{Car}_{S_1} \rightarrow \text{B850}} = \left(1 - \frac{\tau_{S_1}^{\text{LH2}}}{\tau_{S_1}^{\text{Sol}}} \right) \times 100 \quad (1)$$

Table 2. Energy and Lifetime of the Carotenoid S_1 ($2^1A_g^-$) State along with B850* Quenching Rate (if Evident)

carotenoid	N^a	$N_{C=C}$	$N_{C=O}$	environment	S_1 (cm^{-1}) [nm] ^b	$\tau_{S_1}^c$ (ps) RT ^c	$\tau_{S_1}^c$ (ps) 77 K [10 K]	k_q^{-1} (ns) ^d	ref
neurosporene	9	9	0	v.s. ^f	14 170–14 400 [695–706]	21–24	34.8	n.e. ^h	44, 45
									44–47
									45
									this work
spheroidene	10	10	0	v.s.	13 400 [746]	7.7–9.3	11.5	n.e.	44, 49
									33, 48, 50, 51
									45
									this work
lycopene	11	11	0	v.s.	12 500 [800]	4–4.7	3.3	5.9	33
									48, 52
									this work
									33
rhodopin	11	11	0	benzene	12 450 [803]	3.3	3.2	5.9	48
									53
									this work
									45, 53, 54
spirilloxanthin	13	13	0	v.s.	11 350–11 500 [870–881]	1.3–1.7	2.0	1.6	41, 44, 45, 52–56
									45
									24
									this work
diketospirilloxanthin	15	13	2	v.s.	11 000–11 100 [900–909]	0.8	1.2	1.6	24
									24
									24
									this work

^aTotal number of conjugated double bonds ($N = N_{C=C} + N_{C=O}$). ^bEnergy value defined via measuring $S_1 \rightarrow S_2$ energy gap. ^cCarotenoid S_1 ($2^1A_g^-$) state lifetime. ^dB850-to-carotenoid time constant (inverse rate constant) in LH2 assuming that unquenched B850 lifetime is 1.35 ns. ^eRoom temperature. ^fVarious solvents. ^gRb. *sphaeroides* strain. ^hNot evident.

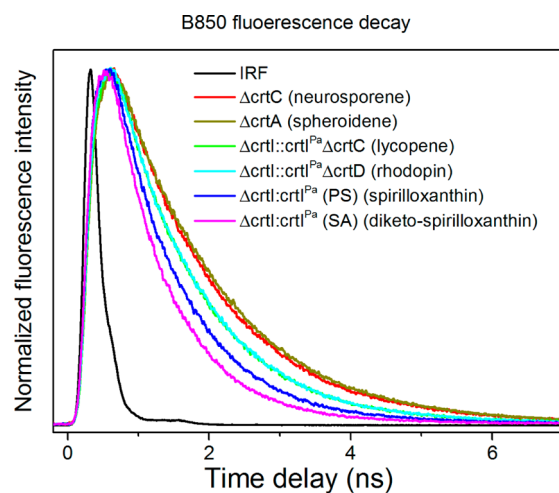


Figure 8. Temporal characteristics of the B850 BChls fluorescence in the LH2 complexes from six *Rb. sphaeroides* strains: Fluorescence decay curves recorded under annihilation free condition after excitation at 590 nm at RT; IRF, instrument response function.

Here $\tau_{S_1}^{LH2}$ and $\tau_{S_1}^{Sol}$ are the lifetimes of the S_1 ($2^1A_g^-$) state in the LH2 and in organic solvent, respectively. Because temporal resolution of the TA measurements precludes precise determination of S_2 ($1^1B_u^+$) state lifetime, the contribution of this state to energy transfer is deduced using the assumption

that the overall yield of energy transfer from carotenoid to B850 ($\Phi_{Car \rightarrow B850}$) is given by the experimental value obtained from comparison of absorbance ($1-T$) and fluorescence–excitation spectra and that this is equal to the yield obtained from analysis of carotenoid excited-state lifetime data. The overall $\Phi_{Car \rightarrow B850}$ is given by eq 2.

$$\Phi_{Car \rightarrow B850} = \Phi_{CarS_2 \rightarrow B850} + (100 - \Phi_{CarS_2 \rightarrow B850} - \Phi_{CarS_2 \rightarrow S^*}) \times \frac{Eff_{CarS_1 \rightarrow B850}}{100} \quad (2)$$

In eq 2, all values are given as percent, and the term in parentheses reflects the fraction of the S_2 ($1^1B_u^+$) state that decays to the S_1 ($2^1A_g^-$) state. Within that term, $\Phi_{CarS_2 \rightarrow S^*}$ is yield of formation of so-called S^* state from the S_2 ($1^1B_u^+$) state. It is generally accepted that the S^* state is formed directly from the S_2 ($1^1B_u^+$) and does not play any significant role in energy transfer to BChl *a* as its role is limited to being a precursor of carotenoid triplet.^{43,57,58} The yield of S^* state formation appears to be similar across all studied LH2 complexes studied here. The value of $\Phi_{CarS_2 \rightarrow S^*}$ is assumed to be 10% in all cases on the basis of the ratio of bleaching of the ground-state absorption associated with the S^* TA signal to the overall bleaching observed immediately after the excitation flash.

The results of this analysis, provided in Table 3, show that actual contribution of the S_1 ($2^1A_g^-$) state in the overall

Table 3. Carotenoid S_1 ($2^1A_g^-$) State Lifetimes and Contributions of Carotenoid Excited States to Energy Transfer to BChl *a*

carotenoid	N^a	$N_{C=C}$	$N_{C=O}$	τ_{S_1} (ps)		Eff _{Car S1→B850} (%) ^d	$\Phi_{Car S1→B850}$ (%) ^e	$\Phi_{Car S2→B850}$ (%) ^f	$\Phi_{Car→B850}$ (%) ^g
				solvent ^b	LH2 ^c				
neurosporene	9	9	0	22.5	1.2	95	27	60	87
spheroidene	10	10	0	8.5	1.4	84	18	70	88
lycopene	11	11	0	4.4	3.4	23	7	59	66
rhodopin	11	11	0	3.3	2.9	12	3	62	65
spirilloxanthin	13	13	0	1.5	1.4	0	0	46	46
diketospirilloxanthin	15	13	2	0.8	1.1	0	0	41	41

^aTotal number of conjugated double bonds ($N = N_{C=C} + N_{C=O}$). ^b S_1 ($2^1A_g^-$) state lifetime in solvent calculated as midrange of literature values (RT) given in Table 2. ^c S_1 ($2^1A_g^-$) state lifetime in LH2 at RT obtained in this work. ^dCarotenoid-to-BChl *a* energy transfer efficiency for S_1 ($2^1A_g^-$) obtained from difference between lifetime in solvent and in LH2; this value is the percentage of S_1 ($2^1A_g^-$) state produced from S_2 ($1^1B_u^+$) that gives energy transfer to B850 calculated via eq 1. ^eThe quantum yield of energy transfer from S_1 ($2^1A_g^-$) to B850; this value is the actual contribution of carotenoid S_1 ($2^1A_g^-$) state to the overall energy transfer (per photon absorbed to produce the S_2 ($1^1B_u^+$) state obtained using eq 2. ^fQuantum yield of energy transfer from the carotenoid S_2 ($1^1B_u^+$) state to B850; this value is the actual contribution of the carotenoid S_2 ($1^1B_u^+$) state to overall energy transfer. ^gOverall carotenoid-to-BChl *a* energy transfer yield obtained from comparison of absorbance ($1-T$) and fluorescence excitation spectra.

$\Phi_{Car→B850}$ is actually not the dominant factor even for carotenoids such as neurosporene for which the $\phi_{CarS1→B850}$ pathway is very efficient in that it comprises a substantial fraction of the S_1 ($2^1A_g^-$) state decay.

The steady-state fluorescence studies reveal trends in the yield of B850 fluorescence yield. This point is shown in Figure 9A, which reveals a nominally linear relationship (red dashed line) of Φ_f and $\Phi_{Car→BChl}$ (Table 1). At first glance, one might not expect a connection between these two quantities because the Φ_f values were obtained using direct excitation of B850 BChl array (and the B800 BChls) in the Q_x band and thus should not be affected by the yield of energy transfer from carotenoid to BChl *a*. Rather one might have expected Φ_f to remain at the ~11% level found for the short-chain carotenoids neurosporene and spheroidene (Figure 9A black dashed line). The results in Figure 9A suggest that the B850 Φ_f is sensitive to one or more carotenoid characteristics that also affect energy transfer to B850. One such property is energy of the carotenoid S_1 ($2^1A_g^-$) excited state (Table 2). Figure 9B shows the relationship between this energy and the B850 Φ_f . The Φ_f value drops as carotenoid S_1 ($2^1A_g^-$) state falls from >13,000 (spheroidene, neurosporene) to ~12 500 cm^{-1} (rhodopin, lycopene) and further still for the two longer-chain carotenoids as the energy descends to the ~11 100 cm^{-1} level for diketospirilloxanthin.

The results in Figure 9A and B suggest that (1) photons absorbed by B850 or B800 in the upper excited states (e.g., Q_x band) do not result in quantitative formation of the lowest (Q_y) excited state of the BChl *a* array (B850*) because of rapid competing energy transfer to the carotenoid and/or (2) B850* itself is quenched by energy transfer to the carotenoid. The latter quenching contribution also would be expected to give rise to a reduction in the B850* excited-state lifetime. In this connection, Table 2 and Figure 9C show that the B850* lifetime is ~1.3 ns for the LH2s with short-chain carotenoids neurosporene ($N = 9$) and spheroidene ($N = 10$) and decreases substantially to ~0.75 ns for the LH2 containing the much longer diketospirilloxanthin ($N = 15$). The data depicted in Figure 9C suggest that quenching of B850* by diketospirilloxanthin is reasonable because the S_1 ($2^1A_g^-$) excited-state energy of this carotenoid (11 100 cm^{-1}) has dropped below that of B850* (11 760 cm^{-1}). The same is true for spirilloxanthin, for which the S_1 ($2^1A_g^-$) energy is 11 300 cm^{-1} and the B850* lifetime is ~0.9 ns. What is surprising is that there is a modest

B850* reduction to ~1.1 ns for lycopene and rhodopin, which have an S_1 ($2^1A_g^-$) energy of ~12 500 cm^{-1} . The latter energy is near that of B800 and the suspected position of the “upper” exciton level of B850* that carries little oscillator strength, the bulk of which is in the “lower” component that gives rise to the B850 band. This upper state has been proposed to serve as an energetic “bridge” for energy flow from the B800 to B850 sets of BChl *a* molecules.⁶⁰

Interestingly, the trends in excited-state lifetime (Figure 9C) and Φ_f (Figure 9A) roughly parallel each other in that in both cases values for lycopene and rhodopin are intermediate between spheroidene (plus neurosporene) and diketospirilloxanthin, with spirilloxanthin slightly above the diketo-analogue. Such trends cannot be explained by thermal repopulation of the upper excited states (e.g., the upper exciton level) of B850*, which should be negligible even at room temperature. Energy flow from the upper exciton states of B850 (or B800) to carotenoid could contribute to the Φ_f reduction trend if sufficiently fast (despite apparent poor dipole–dipole coupling) to compete with relaxation to B850*, but to first order would not contribute to the B850* lifetime reduction because the two exciton levels are normally considered to be discrete states. One possible explanation for these observations is that the B850 and carotenoid excited-state manifolds are tightly coupled and that altering the carotenoid alters the excited-state mixing and thereby affects the B850* photophysical properties more so than might meet the eye from the optical spectra. Another explanation is that carotenoid S_1 ($2^1A_g^-$) state of energies lie lower than placed by comparison of wavelength of the S_1 ($2^1A_g^-$) → S_2 ($1^1B_u^+$) TA feature and the wavelength (energy) of the S_0 ($1^1A_g^-$) → S_2 ($1^1B_u^+$) ground-state absorption band. The accuracy of that method has been debated, as S_1 ($2^1A_g^-$) energies obtained via this TA technique are often somewhat smaller than from the S_1 ($2^1A_g^-$) → S_0 ($1^1A_g^-$) fluorescence measurements by 500–1000 cm^{-1} .⁶¹ Regardless, such considerations do not diminish the fact that the longest carotenoids, because of their low S_1 ($2^1A_g^-$) energies, quench B850*.

In our previous study of two representatives of the engineered *Rb. sphaeroides* LH2 family — those that incorporated carotenoids with long ($N = 13$ –15) conjugation lengths²⁴ — we speculated that a direct quenching of the B850* by carotenoids such as spirilloxanthin and diketospirilloxanthin may occur and seems energetically favorable. However, the B850* lifetimes in that study were obtained

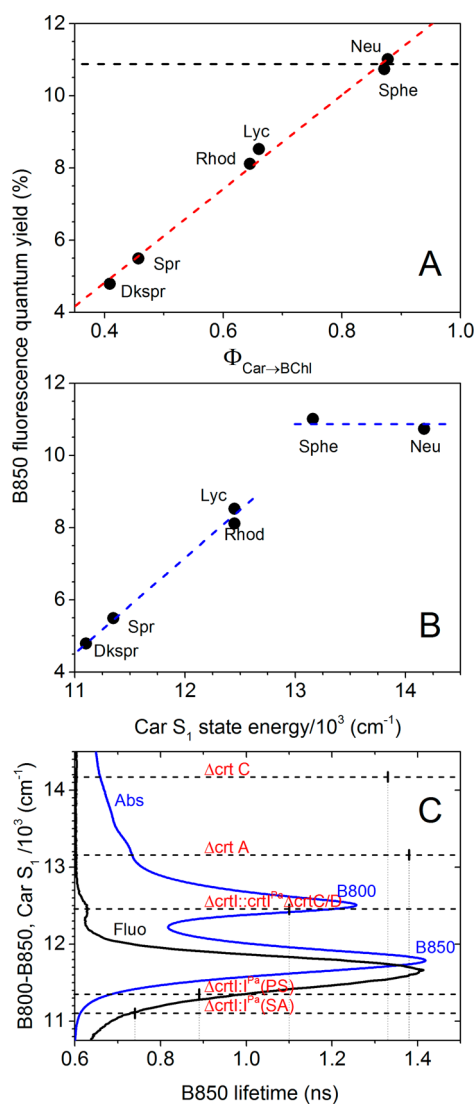


Figure 9. B850 fluorescence quantum yield studies: (A) B850 fluorescence quantum yield as a function $\Phi_{\text{Car} \rightarrow \text{BChl}}$. (B) B850 fluorescence quantum yield as a function of the carotenoid S_1 ($2^1A_g^-$) state energy. (C) Relationship between the B850 fluorescence lifetime, the S_1 ($2^1A_g^-$) excited-state energy of the main carotenoid bound in a particular LH2, and the energies of the B800 and B850 bands. The dotted lines in panels (A) and (B) are guides to the eye.

from TA measurements. In those measurements like those described here on the set of *Rb. sphaeroides* LH2s (in either Tris-LDAO or HEPES-DDM), the B850* lifetime for the longest carotenoids ($N = 13-15$) are consistently somewhat under 1 ns and those for the shortest carotenoids ($N = 9-10$) are consistently somewhat over 1 ns. However, it has been uncertain whether such variations in B850* lifetimes obtained from such TA data indeed reflects carotenoid quenching or arises from differences in time-resolved measurements (e.g., differing contributions of excited-state annihilation) and/or from unforeseen aspects of this unique set of LH2s. The comprehensive studies reported herein have employed the least invasive excited-state monitoring techniques using fluorescence decay with weak excitation flashes. The time-resolved measurements have been complemented by static B850* fluorescence-yield studies (that use weaker excitation) that are sparse in the LH2 literature and that afford the same trends as the B850*

lifetime studies (Table 2). These collective measurements demonstrate that shortening of the B850* lifetime with longer-chain carotenoids is real and most likely arises from direct quenching of the excited state of the B850 BChl *a* array by carotenoid.

Although direct quenching of BChl *a* singlet excited states by carotenoids in protein environments has not been reported previously to our knowledge, such carotenoid-mediated quenching via excitation energy transfer has been seen for the related pigment chlorophyll *a* in representative photosynthetic protein complexes from higher plants such as LHCII⁵⁹ or from cyanobacteria such as IsiA⁶² and in the Hlip proteins.^{63,64} Quenching by excited-state mixing has been suggested in Chl *a* light-harvesting protein as LHCII⁶⁵ and in synthetic carotenoid-tetrapyrrole dyads.^{66,67} It should also be emphasized that direct quenching of B850* by carotenoids in LH2 systems cannot be monitored by recording of the rise and decay of the carotenoid ESA band associated with the S_1 ($2^1A_g^-$) state that serves as the energy quencher, as was possible for the cyanobacterial HliD protein.^{63,64} This is so because the effective concentration of carotenoids in the S_1 ($2^1A_g^-$) state depends on the relative rates of the formation (population) and decay of this excited state. The formation is driven by the B850* quenching rate constant (k_q , Table 2), which is quite small (the process is slow) compared to the extremely large (rapid) S_1 ($2^1A_g^-$) decay. Consequently, the effective concentration of excited carotenoids will be extremely small at a given time in LH2.

CONCLUSIONS

There are two principal conclusions from this study. First, the essential factors that determine electronic communication and thus energy flow between carotenoid and BChl *a* molecules in LH2 complexes are the inherent electronic properties of the carotenoid; polypeptide properties that vary from strain to strain are far less important in regulation of energy transfer between the carotenoids and BChl *a* molecules. Second, if the carotenoid possesses π -electron conjugation that is long enough to afford an S_1 ($2^1A_g^-$) energy comparable to or lower than the S_1 energy of excited BChl-*a* array B850*, quenching of B850* by the carotenoid occurs. In this regard, the S_1 ($2^1A_g^-$) energy of the longer chain carotenoids bearing keto groups (e.g., ketospirilloxanthin and diketospirilloxanthin), is sufficiently low due to the large $N_{C=C}$ (plus $N_{C=O}$) that effects of the protein involving the keto groups will have little consequence.

ASSOCIATED CONTENT

Supporting Information

The Supporting Information is available free of charge on the ACS Publications website at DOI: 10.1021/acs.jpcc.6b03305.

Full references for references with >10 authors (PDF)

AUTHOR INFORMATION

Corresponding Authors

*E-mail: holten@wustl.edu. Tel: 314-935-6502.

*E-mail: niedzwiedzki@wustl.edu. Tel: 314-935-8483.

Present Address

[†]D.J.M.: Marine Biology Section, Department of Biology, University of Copenhagen, Strandpromenaden 5, DK-3000 Helsingør, Denmark.

Notes

The authors declare no competing financial interest.

ACKNOWLEDGMENTS

This research was supported by the Photosynthetic Antenna Research Center (PARC), an Energy Frontier Research Center funded by the U.S. Department of Energy, Office of Science, Office of Basic Energy Sciences under Award Number DE-SC 0001035. That grant supported the growth and isolation of bacterial cells (U.K.) and the static/time-resolved spectroscopy on the LH2 complexes (U.S.). For generation of the mutant strain and initial characterization studies, C.N.H. gratefully acknowledges financial support from the Biotechnology and Biological Sciences Research Council (BBSRC UK), award number BB/M000265/1. C.N.H. was also supported by an Advanced Award 338895 from the European Research Council.

REFERENCES

- (1) Qian, P.; Papiz, M. Z.; Jackson, P. J.; Brindley, A. A.; Ng, I. W.; Olsen, J. D.; Dickman, M. J.; Bullough, P. A.; Hunter, C. N. Three-Dimensional Structure of the *Rhodobacter sphaeroides* RC-LH1-PufX Complex: Dimerization and Quinone Channels Promoted by PufX. *Biochemistry* **2013**, *52*, 7575–7585.
- (2) Cartron, M. L.; Olsen, J. D.; Sener, M.; Jackson, P. J.; Brindley, A. A.; Qian, P.; Dickman, M. J.; Leggett, G. J.; Schulten, K.; Hunter, C. N. Integration of Energy and Electron Transfer Processes in the Photosynthetic Membrane of *Rhodobacter sphaeroides*. *BBA-Bioenergetics* **2014**, *1837*, 1769–1780.
- (3) McDermott, G.; Prince, S. M.; Freer, A. A.; Hawthornthwaite-Lawless, A. M.; Papiz, M. Z.; Cogdell, R. J.; Isaacs, N. W. Crystal Structure of an Integral Membrane Light-Harvesting Complex from Photosynthetic Bacteria. *Nature* **1995**, *374*, 517–521.
- (4) Prince, S. M.; Papiz, M. Z.; Freer, A. A.; McDermott, G.; Hawthornthwaite-Lawless, A. M.; Cogdell, R. J.; Isaacs, N. W. Apoprotein Structure in the LH2 Complex from *Rhodospseudomonas acidophila* Strain 10050: Modular Assembly and Protein Pigment Interactions. *J. Mol. Biol.* **1997**, *268*, 412–423.
- (5) Papiz, M. Z.; Prince, S. M.; Howard, T.; Cogdell, R. J.; Isaacs, N. W. The Structure and Thermal Motion of the B800–850 LH2 Complex from *Rps. acidophila* at 2.0 Å Resolution and 100 K: New Structural Features and Functionally Relevant Motions. *J. Mol. Biol.* **2003**, *326*, 1523–1538.
- (6) Koepke, J.; Hu, X.; Muenke, C.; Schulten, K.; Michel, H. The Crystal Structure of the Light-Harvesting Complex II (B800–850) from *Rhodospirillum molischianum*. *Structure* **1996**, *4*, 581–597.
- (7) Walz, T.; Jamieson, S. J.; Bowers, C. M.; Bullough, P. A.; Hunter, C. N. Projection Structures of Three Photosynthetic Complexes from *Rhodobacter sphaeroides*: LH2 at 6 Å LH1 and RC-LH1 at 25 Å. *J. Mol. Biol.* **1998**, *282*, 833–845.
- (8) Kereiche, S.; Bourinet, L.; Keegstra, W.; Arteni, A. A.; Verbavatz, J. M.; Boekema, E. J.; Robert, B.; Gall, A. The Peripheral Light-Harvesting Complexes from Purple Sulfur Bacteria Have Different 'Ring' Sizes. *FEBS Lett.* **2008**, *582*, 3650–3656.
- (9) Christensen, R. L. The Electronic States of Carotenoids. In *Photochemistry of Carotenoids*; Frank, A. J. et al., Eds.; Kluwer Academic Publishers: Dordrecht, Boston, London, 1999; pp 137–159.
- (10) Cong, H.; Niedzwiedzki, D. M.; Gibson, G. N.; LaFountain, A. M.; Kelsh, R. M.; Gardiner, A. T.; Cogdell, R. J.; Frank, H. A. Ultrafast Time-Resolved Carotenoid to-Bacteriochlorophyll Energy Transfer in LH2 Complexes from Photosynthetic Bacteria. *J. Phys. Chem. B* **2008**, *112*, 10689–10703.
- (11) Polivka, T.; Zigmantas, D.; Herek, J. L.; He, Z.; Pascher, T.; Pullerits, T.; Cogdell, R. J.; Frank, H. A.; Sundstrom, V. The Carotenoid S₁ State in LH2 Complexes from Purple Bacteria *Rhodobacter sphaeroides* and *Rhodospseudomonas acidophila*: S₁ Energies, Dynamics, and Carotenoid Radical Formation. *J. Phys. Chem. B* **2002**, *106*, 11016–11025.
- (12) Rondonuwu, F. S.; Yokoyama, K.; Fujii, R.; Koyama, Y.; Cogdell, R. J.; Watanabe, Y. The Role of the ¹B_u⁻ State in Carotenoid-to-Bacteriochlorophyll Singlet-Energy Transfer in the LH2 Antenna Complexes from *Rhodobacter sphaeroides* G1C, *Rhodobacter sphaeroides* 2.4.1, *Rhodospirillum molischianum* and *Rhodospseudomonas acidophila*. *Chem. Phys. Lett.* **2004**, *390*, 314–322.
- (13) Herzberg, G.; Teller, E. Fluctuation Structure of Electron Transfer in Multiatomic Molecules. *Z. Phys. Chem. B-Chem. E* **1933**, *21*, 410–446.
- (14) Zgierski, M. Z. Herzberg-Teller Interaction and Vibronic Coupling in Molecular-Crystals 0.2. Simple Model with Inclusion of a Frequency Change in Nontotally Symmetric Vibration. *Phys. Status Solidi B* **1974**, *62*, 51–55.
- (15) Hsu, C. P.; Walla, P. J.; Head-Gordon, M.; Fleming, G. R. The Role of the S(1) State of Carotenoids in Photosynthetic Energy Transfer: The Light-Harvesting Complex II of Purple Bacteria. *J. Phys. Chem. B* **2001**, *105*, 11016–11025.
- (16) Damjanovic, A.; Ritz, T.; Schulten, K. The Role of Carotenoids in Photosynthesis. *Biophys. J.* **1999**, *76*, A239.
- (17) Krinsky, N. I. Function. In *Carotenoids*; Isler, O., Guttman, N., Solms, U., Eds.; Birghäuser Verlag: Basel, Switzerland, 1971; p 669.
- (18) Šlouf, V.; Chábera, P.; Olsen, J. D.; Martin, E. C.; Qian, P.; Hunter, C. N.; Polivka, T. Photoprotection in a Purple Phototrophic Bacterium Mediated by Oxygen-Dependent Alteration of Carotenoid Excited-State Properties. *Proc. Natl. Acad. Sci. U. S. A.* **2012**, *109*, 8570–8575.
- (19) Angerhofer, A.; Bornhauser, F.; Gall, A.; Cogdell, R. J. Optical and Optically Detected Magnetic-Resonance Investigation on Purple Photosynthetic Bacterial Antenna Complexes. *Chem. Phys.* **1995**, *194*, 259–274.
- (20) Frank, H. A.; Cogdell, R. J. Carotenoids in Photosynthesis. *Photochem. Photobiol.* **1996**, *63*, 257–264.
- (21) Chi, S. C.; Mothersole, D. J.; Dilbeck, P.; Niedzwiedzki, D. M.; Zhang, H.; Qian, P.; Vasilev, C.; Grayson, K. J.; Jackson, P. J.; Martin, E. C.; et al. Assembly of Functional Photosystem Complexes in *Rhodobacter sphaeroides* Incorporating Carotenoids from the Spirilloxanthin Pathway. *Biochim. Biophys. Acta, Bioenerg.* **2015**, *1847*, 189–201.
- (22) Niedzwiedzki, D. M.; Kobayashi, M.; Blankenship, R. E. Triplet Excited State Spectra and Dynamics of Carotenoids from the Thermophilic Purple Photosynthetic Bacterium *Thermochromatium tepidum*. *Photosynth. Res.* **2011**, *107*, 177–186.
- (23) Niedzwiedzki, D. M.; Bina, D.; Picken, N.; Honkanen, S.; Blankenship, R. E.; Holten, D.; Cogdell, R. J. Spectroscopic Studies of Two Spectral Variants of Light-Harvesting Complex 2 (LH2) from the Photosynthetic Purple Sulfur Bacterium *Allochromatium vinosum*. *BBA-Bioenergetics* **2012**, *1817*, 1576–1587.
- (24) Niedzwiedzki, D. M.; Dilbeck, P. L.; Tang, Q.; Mothersole, D. J.; Martin, E. C.; Bocian, D. F.; Holten, D.; Hunter, C. N. Functional Characteristics of Spirilloxanthin and Keto-Bearing Analogues in Light-Harvesting LH2 Complexes from *Rhodobacter sphaeroides* with a Genetically Modified Carotenoid Synthesis Pathway. *BBA-Bioenergetics* **2015**, *1847*, 640–655.
- (25) Garcia-Asua, G.; Lang, H. P.; Cogdell, R. J.; Hunter, C. N. Carotenoid Diversity: A Modular Role for the Phytoene Desaturase Step. *Trends Plant Sci.* **1998**, *3*, 445–449.
- (26) Vairaprakash, P.; Yang, E.; Sahin, T.; Taniguchi, M.; Krayer, M.; Diers, J. R.; Wang, A.; Niedzwiedzki, D. M.; Kirmaier, C.; Lindsey, J. S.; et al. Extending the Short and Long Wavelength Limits of Bacteriochlorin near-Infrared Absorption Via Dioxo- and Bisimide-Functionalization. *J. Phys. Chem. B* **2015**, *119*, 4382–4395.
- (27) van Stokkum, I. H. M.; Larsen, D. S.; van Grondelle, R. Global and Target Analysis of Time-Resolved Spectra. *Biochim. Biophys. Acta* **2004**, *1657*, 82–104.
- (28) Gall, A.; Cogdell, R. J.; Robert, B. Influence of Carotenoid Molecules on the Structure of the Bacteriochlorophyll Binding Site in Peripheral Light-Harvesting Proteins from *Rhodobacter sphaeroides*. *Biochemistry* **2003**, *42*, 7252–7258.
- (29) Freiberg, A.; Ratsep, M.; Timpmann, K.; Trinkunas, G.; Woodbury, N. W. Self-Trapped Excitons in LH2 Antenna Complexes between 5 K and Ambient Temperature. *J. Phys. Chem. B* **2003**, *107*, 11510–11519.

- (30) Chen, X. H.; Zhang, L.; Weng, Y. X.; Du, L. C.; Ye, M. P.; Yang, G. Z.; Fujii, R.; Rondonuwu, F. S.; Koyama, Y.; Wu, Y. S.; et al. Protein Structural Deformation Induced Lifetime Shortening of Photosynthetic Bacteria Light-Harvesting Complex LH2 Excited State. *Biophys. J.* **2005**, *88*, 4262–4273.
- (31) Monshouwer, R.; Abrahamsson, M.; van Mourik, F.; van Grondelle, R. Superradiance and Exciton Delocalization in Bacterial Photosynthetic Light-Harvesting Systems. *J. Phys. Chem. B* **1997**, *101*, 7241–7248.
- (32) Pflock, T.; Dezi, M.; Venturoli, G.; Cogdell, R. J.; Kohler, J.; Oellerich, S. Comparison of the Fluorescence Kinetics of Detergent-Solubilized and Membrane-Reconstituted LH2 Complexes from *Rps. acidophila* and *Rb. sphaeroides*. *Photosynth. Res.* **2008**, *95*, 291–298.
- (33) Horvin Billsten, H.; Herek, J. L.; Garcia-Asua, G.; Hashoj, L.; Polivka, T.; Hunter, C. N.; Sundstrom, V. Dynamics of Energy Transfer from Lycopene to Bacteriochlorophyll in Genetically-Modified LH2 Complexes of *Rhodobacter sphaeroides*. *Biochemistry* **2002**, *41*, 4127–4136.
- (34) Bopp, M. A.; Jia, Y. W.; Li, L. Q.; Cogdell, R. J.; Hochstrasser, R. M. Fluorescence and Photobleaching Dynamics of Single Light-Harvesting Complexes. *Proc. Natl. Acad. Sci. U. S. A.* **1997**, *94*, 10630–10635.
- (35) Merlin, J. C. Resonance Raman-Spectroscopy of Carotenoids and Carotenoid-Containing Systems. *Pure Appl. Chem.* **1985**, *57*, 785–792.
- (36) Koyama, Y.; Takatsuka, I.; Nakata, M.; Tasumi, M. Raman and Infrared-Spectra of the all-*trans*, 7-*cis*, 9-*cis*, 13-*cis* and 15-*cis* Isomers of β -carotene - Key Bands Distinguishing Stretched or Terminal-Bent Configurations from Central-Bent Configurations. *J. Raman Spectrosc.* **1988**, *19*, 37–49.
- (37) Mendes-Pinto, M. M.; Sansiaume, E.; Hashimoto, H.; Pascal, A. A.; Gall, A.; Robert, B. Electronic Absorption and Ground State Structure of Carotenoid Molecules. *J. Phys. Chem. B* **2013**, *117*, 11015–11021.
- (38) Robert, B. Resonance Raman Studies in Photosynthesis - Chlorophyll and Carotenoid Molecules. In *Biophysical Techniques in Photosynthesis*; Kluwer Academic Publishers: New York, Boston, Dordrecht, London, Moscow, 1996; pp 161–174.
- (39) Cogdell, R. J.; Hipkins, M. F.; Macdonald, W.; Truscott, T. G. Energy-Transfer between the Carotenoid and the Bacteriochlorophyll within the B800–850 Light-Harvesting Pigment-Protein Complex of *Rhodospseudomonas sphaeroides*. *Biochim. Biophys. Acta* **1981**, *634*, 191–202.
- (40) van Grondelle, R.; Kramer, H. J. M.; Rijgersberg, C. P. Energy Transfer in the B800–850-Carotenoid Light-Harvesting Complex of Various Mutants of *Rhodospseudomonas sphaeroides* and of *Rhodospseudomonas capsulata*. *Biochim. Biophys. Acta* **1982**, *682*, 208–215.
- (41) Gradinaru, C. C.; Kennis, J. T.; Papagiannakis, E.; van Stokkum, I. H.; Cogdell, R. J.; Fleming, G. R.; Niederman, R. A.; van Grondelle, R. An Unusual Pathway of Excitation Energy Deactivation in Carotenoids: Singlet-to-Triplet Conversion on an Ultrafast Timescale in a Photosynthetic Antenna. *Proc. Natl. Acad. Sci. U. S. A.* **2001**, *98*, 2364–2369.
- (42) Papagiannakis, E.; Kennis, J. T. M.; van Stokkum, I. H. M.; Cogdell, R. J.; van Grondelle, R. An Alternative Carotenoid-to-Bacteriochlorophyll Energy Transfer Pathway in Photosynthetic Light Harvesting. *Proc. Natl. Acad. Sci. U. S. A.* **2002**, *99*, 6017–6022.
- (43) Papagiannakis, E.; Das, S. K.; Gall, A.; van Stokkum, I. H. M.; Robert, B.; van Grondelle, R.; Frank, H. A.; Kennis, J. T. M. Light Harvesting by Carotenoids Incorporated into the B850 Light-Harvesting Complex from *Rhodobacter sphaeroides* R-26.1: Excited-State Relaxation, Ultrafast Triplet Formation, and Energy Transfer to Bacteriochlorophyll. *J. Phys. Chem. B* **2003**, *107*, S642–S649.
- (44) Niedzwiedzki, D.; Kosciielecki, J. F.; Cong, H.; Sullivan, J. O.; Gibson, G. N.; Birge, R. R.; Frank, H. A. Ultrafast Dynamics and Excited State Spectra of Open-Chain Carotenoids at Room and Low Temperatures. *J. Phys. Chem. B* **2007**, *111*, S984–S998.
- (45) Niedzwiedzki, D. M.; Sandberg, D. J.; Cong, H.; Sandberg, M. N.; Gibson, G. N.; Birge, R. R.; Frank, H. A. Ultrafast Time-Resolved Absorption Spectroscopy of Geometric Isomers of Carotenoids. *Chem. Phys.* **2009**, *357*, 4–16.
- (46) Zhang, J. P.; Inaba, T.; Watanabe, Y.; Koyama, Y. Excited-State Dynamics among the $1B_u^+$, $1B_u^-$ and $2A_g^-$ States of all-*trans*-Neurosporene as Revealed by near-Infrared Time-Resolved Absorption Spectroscopy. *Chem. Phys. Lett.* **2000**, *332*, 351–358.
- (47) Rondonuwu, F. S.; Watanabe, Y.; Fujii, R.; Koyama, Y. A First Detection of Singlet to Triplet Conversion from the $1^1B_u^-$ to the 1^3A_g State and Triplet Internal Conversion from the 1^3A_g to the 1^3B_u State in Carotenoids: Dependence on the Conjugation Length. *Chem. Phys. Lett.* **2003**, *376*, 292–301.
- (48) Zhang, J. P.; Fujii, R.; Qian, P.; Inaba, T.; Mizoguchi, T.; Onaka, K.; Watanabe, Y.; Nagae, H.; Koyama, Y. Mechanism of the Carotenoid-to-Bacteriochlorophyll Energy Transfer Via the S_1 State in the LH2 Complexes from Purple Bacteria. *J. Phys. Chem. B* **2000**, *104*, 3683–3691.
- (49) Polivka, T.; Zigmantas, D.; Frank, H. A.; Bautista, J. A.; Herek, J. L.; Koyama, Y.; Fujii, R.; Sundstrom, V. Near-Infrared Time-Resolved Study of the S_1 State Dynamics of the Carotenoid Spheroidene. *J. Phys. Chem. B* **2001**, *105*, 1072–1080.
- (50) Pendon, Z. D.; Gibson, G. N.; van der Hoef, I.; Lugtenburg, J.; Frank, H. A. Effect of Isomer Geometry on the Steady-State Absorption Spectra and Femtosecond Time-Resolved Dynamics of Carotenoids. *J. Phys. Chem. B* **2005**, *109*, 21172–21179.
- (51) Frank, H. A.; Farhoosh, R.; Gebhard, R.; Lugtenburg, J.; Gosztola, D.; Wasielewski, M. R. The Dynamics of the S_1 Excited-States of Carotenoids. *Chem. Phys. Lett.* **1993**, *207*, 88–92.
- (52) Fujii, R.; Inaba, T.; Watanabe, Y.; Koyama, Y.; Zhang, J. P. Two Different Pathways of Internal Conversion in Carotenoids Depending on the Length of the Conjugated Chain. *Chem. Phys. Lett.* **2003**, *369*, 165–172.
- (53) Niedzwiedzki, D. M.; Fuciman, M.; Kobayashi, M.; Frank, H. A.; Blankenship, R. E. Ultrafast Time-Resolved Spectroscopy of the Light-Harvesting Complex 2 (LH2) from the Photosynthetic Bacterium *Thermochromatium tepidum*. *Photosynth. Res.* **2011**, *110*, 49–60.
- (54) Papagiannakis, E.; van Stokkum, I. H. M.; van Grondelle, R.; Niederman, R. A.; Zigmantas, D.; Sundstrom, V.; Polivka, T. A near-Infrared Transient Absorption Study of the Excited-State Dynamics of the Carotenoid Spirilloxanthin in Solution and in the LH1 Complex of *Rhodospirillum rubrum*. *J. Phys. Chem. B* **2003**, *107*, 11216–11223.
- (55) Nishimura, K.; Rondonuwu, F. S.; Fujii, R.; Akahane, J.; Koyama, Y.; Kobayashi, T. Sequential Singlet Internal Conversion of $1B_u^+ \rightarrow 3A_g^- \rightarrow 1B_u^- \rightarrow 2A_g^- \rightarrow 1A_g^-$ Ground in all-*trans*-Spirilloxanthin Revealed by Two-Dimensional Sub-5-fs Spectroscopy. *Chem. Phys. Lett.* **2004**, *392*, 68–73.
- (56) Okamoto, H.; Ogura, M.; Nakabayashi, T.; Tasumi, M. Sub-Picosecond Excited-State Dynamics of a Carotenoid (Spirilloxanthin) in the Light-Harvesting Systems of *Chromatium vinosum*. Relaxation Process from the Optically Allowed S_2 State. *Chem. Phys.* **1998**, *236*, 309–318.
- (57) Papagiannakis, E.; van Stokkum, I. H.; Vengris, M.; Cogdell, R. J.; van Grondelle, R.; Larsen, D. S. Excited-State Dynamics of Carotenoids in Light-Harvesting Complexes. 1. Exploring the Relationship between the S_1 and S^* States. *J. Phys. Chem. B* **2006**, *110*, S727–S736.
- (58) Papagiannakis, E.; Kennis, J. T.; van Stokkum, I. H.; Cogdell, R. J.; van Grondelle, R. An Alternative Carotenoid-to-Bacteriochlorophyll Energy Transfer Pathway in Photosynthetic Light Harvesting. *Proc. Natl. Acad. Sci. U. S. A.* **2002**, *99*, 6017–6022.
- (59) Ruban, A. V.; Berera, R.; Iliaia, C.; van Stokkum, I. H. M.; Kennis, J. T. M.; Pascal, A. A.; van Amerongen, H.; Robert, B.; Horton, P.; van Grondelle, R. Identification of a Mechanism of Photoprotective Energy Dissipation in Higher Plants. *Nature* **2007**, *450*, S75–S78.
- (60) Sauer, K.; Cogdell, R. J.; Prince, S. M.; Freer, A.; Isaacs, N. W.; Scheer, H. Structure-Based Calculations of the Optical Spectra of the LH2 Bacteriochlorophyll-Protein Complex from *Rhodospseudomonas acidophila*. *Photochem. Photobiol.* **1996**, *64*, S64–S76.

(61) Polivka, T.; Sundstrom, V. Ultrafast Dynamics of Carotenoid Excited States-from Solution to Natural and Artificial Systems. *Chem. Rev.* **2004**, *104*, 2021–2071.

(62) Berera, R.; van Stokkum, I. H. M.; d'Haene, S.; Kennis, J. T. M.; van Grondelle, R.; Dekker, J. P. A Mechanism of Energy Dissipation in Cyanobacteria. *Biophys. J.* **2009**, *96*, 2261–2267.

(63) Staleva, H.; Komenda, J.; Shukla, M. K.; Slouf, V.; Kana, R.; Polivka, T.; Sobotka, R. Mechanism of Photoprotection in the Cyanobacterial Ancestor of Plant Antenna Proteins. *Nat. Chem. Biol.* **2015**, *11*, 287–291.

(64) Niedzwiedzki, D. M.; Tronina, T.; Liu, H.; Staleva, H.; Komenda, J.; Sobotka, R.; Blankenship, R. E.; Polivka, T. Carotenoid-Induced Non-Photochemical Quenching in the Cyanobacterial Chlorophyll Synthase-Hlic/D Complex. *BBA-Bioenergetics* **2016**, DOI: [10.1016/j.bbabi.2016.04.280](https://doi.org/10.1016/j.bbabi.2016.04.280).

(65) Bode, S.; Quentmeier, C. C.; Liao, P. N.; Hafi, N.; Barros, T.; Wilk, L.; Bittner, F.; Walla, P. J. On the Regulation of Photosynthesis by Excitonic Interactions between Carotenoids and Chlorophylls. *Proc. Natl. Acad. Sci. U. S. A.* **2009**, *106*, 12311–12316.

(66) Berera, R.; Herrero, C.; van Stokkum, I. H. M.; Vengris, M.; Kodis, G.; Palacios, R. E.; van Amerongen, H.; van Grondelle, R.; Gust, D.; Moore, T. A.; et al. A Simple Artificial Light-Harvesting Dyad as a Model for Excess Energy Dissipation in Oxygenic Photosynthesis. *Proc. Natl. Acad. Sci. U. S. A.* **2006**, *103*, 5343–5348.

(67) Kloz, M.; Pillai, S.; Kodis, G.; Gust, D.; Moore, T. A.; Moore, A. L.; van Grondelle, R.; Kennis, J. T. M. Carotenoid Photoprotection in Artificial Photosynthetic Antennas. *J. Am. Chem. Soc.* **2011**, *133*, 7007–7015.